Neutrophil- and Myeloperoxidase-Mediated Metabolism of Reduced Nimesulide: Evidence for Bioactivation

Min Yang,[†] Mahendra D. Chordia,[†] Fengping Li,[†] Tao Huang,[†] Joel Linden,[‡] and Timothy L. Macdonald*,[†]

Department of Chemistry and Cardiovascular Research Center, University of Virginia, Charlottesville, Virginia 22904, United States

Received April 24, 2010

Nimesulide, a widely used nonsteroidal anti-inflammatory drug (NSAID), has been associated with rare idiosyncratic hepatotoxicity. The chemical mechanisms underlying the liver injury remain unknown. We have undertaken the detailed study of the metabolic pathways of nimesulide in an effort to identify potential reactive metabolites. A previous report from this laboratory has demonstrated that one of the known nimesulide metabolites, termed reduced nimesulide (**M1**), is further bioactivated by human liver microsomes (HLMs) to form a reactive diiminoquinone species **M2**. The formation of **M2** was confirmed indirectly by trapping with *N*-acetylcysteine (NAC). The aim of this study was to explore the fate of **M1** in an inflammatory environment created by the recruitment of leukocytes. Leukocytes upon activation produce hydrogen peroxide (H_2O_2) and other myeloperoxidase (MPO) products, such as hypochlorous acid (HOCl), that are capable of metabolite oxidation. We demonstrate here that the reduced nimesulide, **M1**, undergoes a facile oxidation with activated neutrophils or with MPO in the presence of H_2O_2 or HOCl to produce a variety of reactive as well as stable metabolites. One major metabolite, **M3**, was also produced by HLM as determined by trapping with NAC. Other metabolites, for example, **M6**, **M8**, and **M9**, were unique to the myeloperoxidase, because of their mode of formation from activation of the amino group of reduced nimesulide. The structures of some of these reactive metabolites were proposed on the basis of liquid chromatography−tandem mass spectrometry analyses and established by their comparison with synthetic standards. Metabolite **M6** is interesting because it provides clear evidence of amine activation and indicates the potential of the reactive intermediate of **M1** to conjugate with protein nucleophiles. In summary, our results demonstrate that a known nimesulide metabolite could be bioactivated by MPO through a pathway distinct from HLM-mediated pathways and that the generation of reactive species by the MPO-mediated bioactivation pathway at the site of inflammation may contribute to the toxicity associated with nimesulide.

Introduction

Nimesulide, a nonsteroidal anti-inflammatory drug (NSAID)[1] with selectivity for cyclooxygenase 2 (COX-2), has been associated with idiosyncratic hepatotoxicity (*1*−*5*). The use of nimesulide has been abandoned in Finland and Spain because of its relatively strong adverse effects and hepatotoxicity (*6*), although it remains on the market in many other countries. The molecular mechanisms of idiosyncratic liver injury associated with nimesulide are unknown, and there is no very good animal model for exploring the mechanism. However, evidence that implicates hepatic metabolism and disposition of nimesulide and its metabolites as playing a pivotal role in toxicity has been presented (*7*). In an effort to uncover potential reactive species that could play roles in its idiosyncratic toxicity, we have undertaken a program to elucidate the complete metabolic outcome of nimesulide and to survey many of the relevant enzymes associated with bioactivation of nimesulide and its metabolites.

A number of human nimesulide urinary metabolites have been identified and characterized, including hydroxynimesulide [**A** (∼18%)] and a series of metabolites in which the nitro group has been reduced and N-acetyated and the aromatic rings have been hydroxylated [**B** (<0.5%), **C** (∼19%), **M1** (0.72%), and **M1-OH** (3%)] (Figure 1) (*8*). Our lab recently reported detection and characterization of a reactive metabolite, diiminoquinone, from the metabolites of nimesulide **M1** and **M1-OH** by P450-mediated bioactivation (*9*). The diiminoquinone species was difficult to observe but was highly susceptible to conjugation with proteins as demonstrated with human serum albumin (HSA). The aromatic amine group in **M1** and **M1-OH** is presumably prone to oxidation because of their highly electron rich nature. Oxidative enzymes, such as monoamine oxidase MAO and MPO (*10*−*14*), are known to activate primary aromatic amines to generate reactive hydroxyl amine, nitroso, nitrenium ion, and nitrene metabolites. These N-oxidized reactive metabolites are associated with idiosyncratic drug reactions (*15*). In addition, the phenolic metabolites of nimesulide are also susceptible to further oxidation in generating reactive quinone species, although conversion to the phenolic sulfate or glucuronide is possible.

* To whom correspondence should be addressed: Department of Chemistry, University of Virginia, McCormick Road, Charlottesville, VA 22904. Phone: (434) 924-7718. E-mail: tlm@virginia.edu.

[†] Department of Chemistry.

[‡] Cardiovascular Research Center.

[1] Abbreviations: COX-2, cyclooxygenase 2; DIEA, diisopropylethylamine; DMSO, dimethyl sulfoxide; ESI-MS, electrospray ionization mass spectrometry; HBTU, *O*-benzotriazole-*N*,*N*,*N*′,*N*′-tetramethyluronium hexafluorophosphate; IDRs, idiosyncratic drug reactions; MPO, myeloperoxidase; NAC, *N*-acetylcysteine; NSAIDs, nonsteroidal anti-inflammatory drugs; PBS, phosphate-buffered saline; PDA, photodiode array; PMA, phorbol 12-myristate 13-acetate; t_R, retention time.

10.1021/tx1001496
Published on Web 10/12/2010

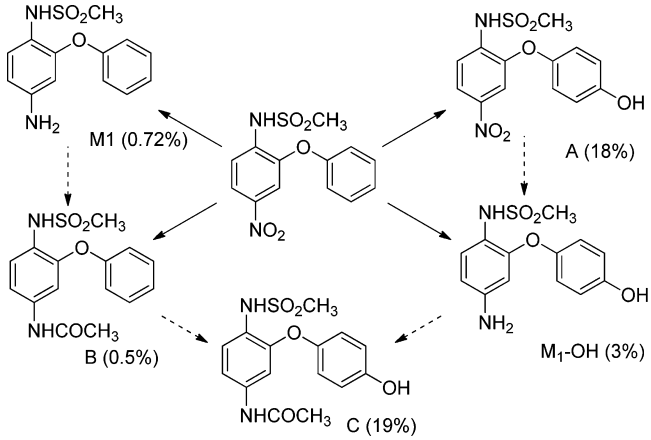

Figure 1. Well-defined metabolites of nimesulide from human urine.

Scheme 1. Proposed Amine Activation of Reduced Nimesulide by Neutrophils and MPO

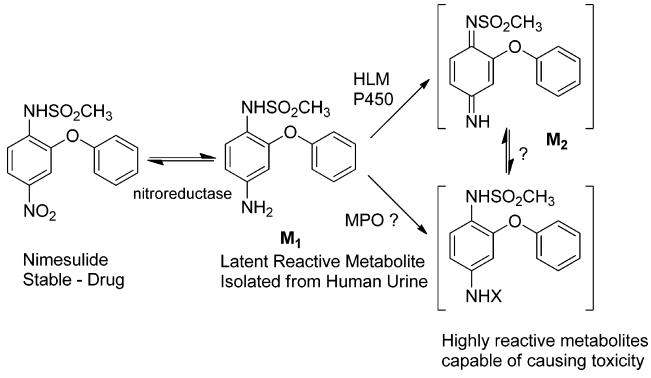

We hypothesized that the reduced nimesulide metabolite **M1** has the potential for bioactivation of the aromatic primary amine group to generate a highly reactive diiminoquinone/*N*-hydroxide electrophilic species by activated neutrophils and/or MPO under inflammatory conditions (Scheme 1). Generation of reactive oxygen species by activated neutrophils is a hallmark of inflammation, and previous studies have demonstrated that activated neutrophils can oxidize some aromatic amine-containing drugs and generate reactive species, as described for procainamide and clozapin (*16*). Thus, MPO has been implicated in the idiosyncratic drug reactions of a number of drugs (*17*−*21*). The aim of this study was to explore the fate of reduced nimesulide in an inflammatory environment that might be encountered in the therapeutic setting. We hypothesized that the metabolism of nimesulide in the liver may generate low levels of damage and inflammation that could be amplified by recruitment of neutrophils and that this altered situation may trigger a toxic response if unchecked.

Experimental Procedures

Chemicals and Instruments. Nimesulide (analytical grade, >95% pure) was procured from Toronto Research Chemicals, Inc. (Toronto, ON). Dichloroamine B was purchased from TCI America (Portland, OR). Human liver microsomes (HLMs) (pooled from 50 livers) and cDNA-expressed human P450 enzymes expressed from either baculovirus-infected insect cells or human lymphoblast cells were purchased from BD Gentest Corp. (Woburn, MA). MPO (from human leukocyte, 220 units/mg of protein) was obtained from Calbiochem (La Jolla, CA). HRP (type X, 291 units/mg of protein) was purchased from Sigma Chemical Corp. (St. Louis, MO). All other reagents, purchased from Sigma or Aldrich (Milwaukee, WI), were of the highest grade available unless otherwise noted. Reverse phase C_{18} preparative TLC plates (250 μm, 20 cm × 20 cm, w/UV 254) were obtained from Sorbent Technology (Atlanta, GA). ^{1}H NMR spectra of the synthesized metabolite were recorded on a Varian 300 MHz spectrometer using standard parameters; chemical shifts are reported in parts per million in reference to residual nondeuterated solvent, and coupling constants are reported in hertz. HPLC-MS and HPLC-MS/MS were performed on a Shimadzu (Columbia, MD) CBM-20A HPLC system equipped with a Thermo-Finnigan (San Jose, CA) LTQ ion trap mass spectrometer with electrospray ionization (ESI). Data were processed using Xcalibur version 1.4.

Purification of the synthesized compounds was conducted on an HPLC system consisting of a Varian Prostar system equipped with a PDA detector, a Grace Appollo C18 column [5 μm, 250 mm × 10 mm (inside diameter)] with a Phenomenex C18 Security Guard cartridge system (10 mm × 10 mm inside diameter), and a Varian Model 701 fraction collector.

Neutrophil Isolation. Fresh human neutrophils were isolated from heparinized (10 units/mL) venous blood using the one-step Ficoll-Hypaque separation technique (*22*) to afford ∼98% pure neutrophils with ≥95% viability as determined with tryptan blue dye. Before incubation with nimesulide or **M1**, the neutrophils were washed three times with Hank's balanced salt solution (HBSS) and heparin (10 units/mL) and resuspended in HA buffer (HBSS containing 0.1% HSA). The neutrophils were kindly provided by R. Grabowska.

Incubations of Nimesulide and Reduced Nimesulide with Neutrophils. To a suspension of neutrophils (∼5.0 million/mL) in HA buffer (3 mL) were added 100 μM **M1** or nimesulide, 5 mM NAC, and PMA (120 ng in 1.2 mL of DMSO). The suspension was incubated at 37 °C for 60 min. After incubation, the suspension was centrifuged at 14000*g* for 10 min, and the supernatant was collected and lyophilized to dryness overnight. The residual samples were redissolved in H_2O and CH_3CN (50:50, 100 μL), and 15 μL samples were injected into the liquid chromatograph for analysis of the metabolite by MS data. In the control experiments, vehicle DMSO replaced the solution of PMA and **M1**.

Incubations of Nimesulide and Reduced Nimesulide with MPO. The incubations containing MPO (1 unit/mL), 100 μM **M1** or nimesulide, and 0.4 M KCl in 0.1 M potassium phosphate buffer (pH 7.4) were performed either with or without NAC (5 mM) in a dry-air bath at 37 °C for 60 min. The reaction was initiated by addition of H_2O_2 (0.22 mM) and terminated by the addition of an equal volume of ice-cold CH_3CN, vortex-mixed, and centrifuged at 14000*g* for 5 min. The resulting supernatant was used for all successive LC−MS and LC−MS/MS analysis. Incubations that lacked MPO, H_2O_2, **M1**, or NAC served as negative controls.

Oxidation of M1 by HOCl. A solution of 1 mM **M1**, 5 mM NAC, and an aqueous solution of 1.6 mM NaOCl were added to an aqueous solution of methanol acidified with 1 mM HCl. The reaction was performed at 0 °C for 2 h. Reaction mixtures that lacked **M1** and NAC served as negative controls. The resulting mixtures were analyzed by LC−MS under the conditions described above.

Identification of Metabolites. Metabolites were identified by positive electrospray LC−MS/MS analysis. A Luna C_{18} reversed phase column (2.0 mm × 150 mm) (Phenomenex, Torrance, CA) was used to separate the samples. The HPLC flow rate was 0.2 mL/min. The mobile phases were methanol (solvent A) and 0.1% formic acid (solvent B). The gradient conditions were as follows: 98% solvent B decreasing to 0% for 20 min and staying at 0% for an additional 10 min. These HPLC conditions were used throughout the experiments. Full parameters for ESI-MS were set as follows: heated capillary temperature of 200 °C, spray voltage of 5 kV, capillary voltage of 43 V, sheath gas flow rate of 25 units, and auxiliary gas flow rate of 3 units.

Chemical Synthesis of Metabolites. (1) Synthesis of 4-Amino-2-phenoxymethanesulfonanilide (reduced nimesulide) and NAC Adduct M3. The detailed synthetic procedures and characterization data for **M1** and **M3** have been reported previously (*9*).

(2) Synthesis of *S*-Oxide M4 and Sulfone. A solution of **M3** (5.0 mg, 0.114 mmol) in CH_2Cl_2 (1.0 mL) was cooled to −70 °C in a cold bath (acetone, dry ice); to this solution was added a premixed cold solution of trifluoroacetic acid and H_2O_2 (9:1, 20.0 μL), and the reaction mixture was stirred at that temperature and allowed to warm to 0 °C overnight. The mixture was then diluted with CH_2Cl_2 (5.0 mL) and evaporated under reduced pressure. The crude material was analyzed by LC−MS analysis as well as by ^{1}H NMR to indicate that oxidation indeed ensued at the sulfur atom to produce ions at *m*/*z* 456 and 472. Further purification of the materials eluting as ions at *m*/*z* 456 and 472 was conducted using semipreparative HPLC. The mobile phase consisted of solvent A (0.1% TFA in water) and solvent B (0.1% TFA in 80% aqueous acetonitrile). The gradient was as follows: 0 min, 30% B; 12 min, 47% B; 14 min, 47% B; 18 min, 54% B; 19 min, 100% B; 20 min, 30% B; 22 min, 30% B. The flow rate was 3 mL/min. The effluent was monitored at 254 nm with a PDA detector. The ion at *m*/*z* 456 was collected with a retention time at 11.7 min. The collected fractions were combined and lyophilized to dryness. The **M4** fraction was 0.6 mg and was further characterized by ^{1}H NMR. The ^{1}H NMR data indicated it is a mixture of diastereomers of the sulfoxide. The compound at *m*/*z* 472 was characterized by LC−MS and assigned the structure of sulfone: ^{1}H NMR (CD_3OD) δ 1.98 and 2.02 (s, 3H, $COCH_3$), 2.97 and 2.98 (s, CH_3, SO_2CH_3), 3.80 (m, 2H, CH_2-S), 4.57 (m, 1H, CH-N), 6.17 (s, 1H, ArH), 7.15 (dd, J = 9 and 3.0, 2H, O-ArH), 7.24 (t, J = 9, 1H, O-ArH), 7.39 (d, J = 3.0, 1H), 7.45 (dd, 2H, ArH).

(3) Synthesis of Metabolite M6. A homogeneous mixture of reduced nimesulide **M1** (69.5 mg, 0.25 mmol), oxidized *N*-acetylcysteine (162.0 mg, 0.5 mmol), HBTU (189.7 mg, 0.5 mmol), and DIEA (645 mg, 5 mmol) in dry CH_3CN (2.5 mL) was stirred overnight at room temperature. The reaction mixture was diluted with a 15 mL (2:1 CH_2Cl_2/EtOAc) solution, transferred to a separatory funnel, and washed with diluted 1 M HCl (3 × 5 mL). The organic layer then washed with water and finally with brine (5 mL each). Concentration of the organic layer under reduced pressure yielded crude material. Further purification of the synthesized **M6** was conducted using semipreparative HPLC. The mobile phase consisted of solvent A (water) and solvent B (acetonitrile). The gradient was as follows: 0 min, 0% B; 20 min, 100% B; 25 min, 100% B; 26 min, 0% B; 30 min, 0% B. The flow rate was 3 mL/min. The effluent was monitored at 254 nm with a UV detector. Fractions containing **M6** were collected at a retention time of 16.8 min. The fractions were combined and lyophilized to dryness (36.0 mg). **M6** was further characterized by ^{1}H NMR and ^{13}C NMR: ^{1}H NMR (CD_3OD) δ 1.96 (s, 3H, $COCH_3$), 1.97 (s, 3H, $COCH_3$), 2.92 (m, 2H, CH_2-S), 2.94 (s, 3H, SO_2CH_3), 3.21 (m, 2H, CH_2-S), 4.71 (m, 2H, CH-N), 7.08 (d, J = 9, 2H, O-ArH), 7.17 (t, J = 9, 1H, O-ArH), 7.28 (m, 2H, ArH), 7.38 (d, J = 9, 2H, O-ArH), 7.43 (d, J = 9, 1H, ArH); ^{13}C NMR (CD_3OD) δ 22.6, 40.3, 41.3, 54.9, 111.3, 116.2, 120.7 (×2), 125.2, 125.5, 128.0, 131.3 (×2), 138.6, 152.2, 157.6, 170.8, 173.6.

Reaction of Reduced Nimesulide with Dichloroamine B. To the cold (0 °C) solution of reduced nimesulide **M1** (5.6 mg, 0.02 mmol) in CH_2Cl_2 (1.0 mL) was added dichloroamine B (4.5 mg, 0.02 mmol), and the mixture was stirred at that temperature for 12 h. The mixture was analyzed by LC−MS analysis for formation of metabolites. Three compounds were detected at *m*/*z* 313 (monochloro compound), *m*/*z* 347 (dichloro compound), and *m*/*z* 555 (dimer of reduced nimesulide). The mixture was separated by preparative HPLC. The fractions at 18.35 and 20.09 min for **M7** and **M8**, respectively, were collected and concentrated under lyophilized conditions.

M7: ^{1}H NMR (CD_3OD) δ 3.02 (s, 3H, SO_2CH_3), 3.36 (s, 3H, SO_2CH_3), 6.23 (s, 1H, ArH), 6.27 (d, J = 1, 1H, ArH), 6.56 (dd, J = 3 and 9, 1H, ArH), 7.10 (d, J = 6, 4H, O-ArH), 7.19 (d, J = 6, 2H, O-ArH), 7.41 (dd, J = 3 and 9, 4H, O-ArH), 7.48 (d, J = 3 and 9, 1H, O-ArH), 7.72 (s, 1H, ArH); ^{13}C NMR (CD_3OD) δ 105.27, 106.27, 112.88, 117.64, 118.29, 121.24, 121.82, 122.24, 125.73, 126.16, 128.53, 130.12, 131.31, 131.43, 132.81, 146.62, 148.47, 154.96, 156.57, 157.27.

M8: ^{1}H NMR (CD_3OD) δ 2.91 (s, 3H, $COCH_3$), 6.34 (s, 1H, ArH), 7.08 (d, J = 9, 2H, O-ArH), 7.17 (t, J = 9 and 1.5, 1H, O-ArH), 7.30 (s, 1H, ArH), 7.40 (t, J = 9 and 1.5, 2H, O-ArH).

Inactivation of MPO by M1. A solution containing 0.1 M potassium phosphate buffer (pH 7.4), 0.4 M KCl, 10 μM **M1**, and 1 unit/mL MPO was incubated at 37 °C, and the reaction was initiated by the addition of H_2O_2 (0.22 mM). Control incubations were performed in the absence of **M1**. After preincubation for 15 min, 100 μM procainamide was added to the preincubation reaction

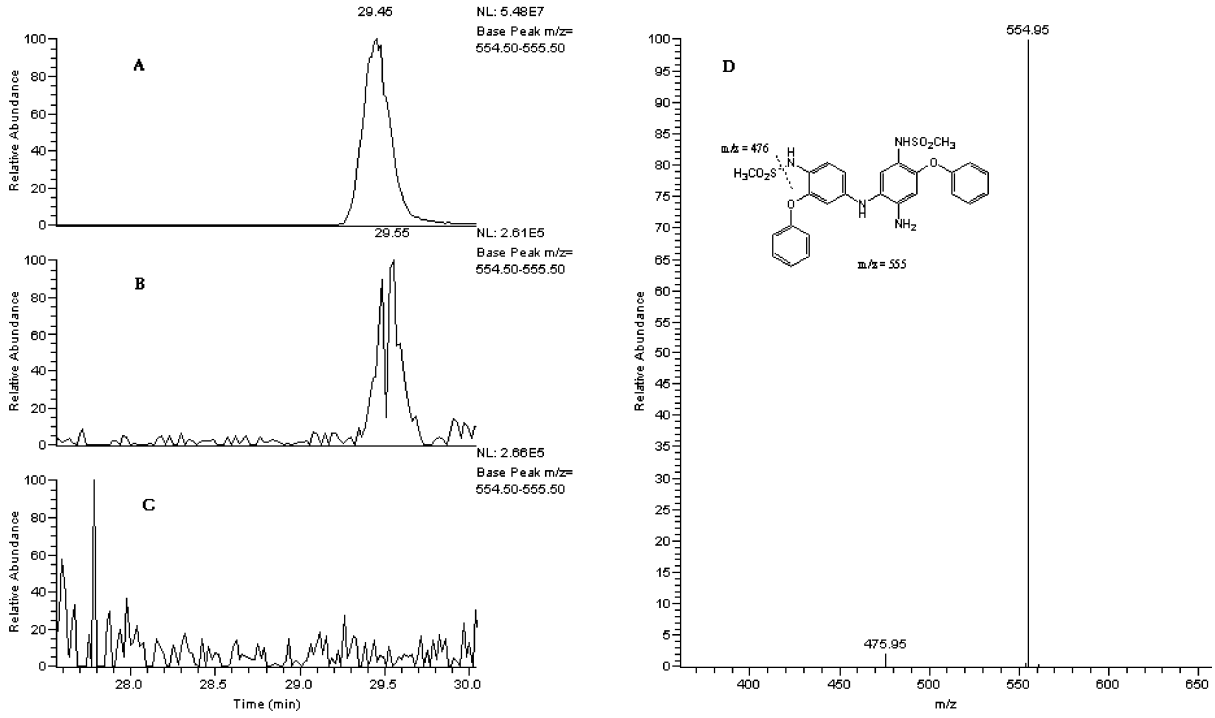

Figure 2. Identification of **M7** (*m*/*z* 555). (A) LC−MS chromatogram of synthetic standard **M7** with $[MH]^+$ extracted for the ion at *m*/*z* 555. (B) LC−MS chromatogram of **M7** at *m*/*z* 555 in MPO and **M1** incubation solutions. (C) LC−MS chromatogram of **M7** in HLM and **M1** reaction product. (D) Full LC−MS/MS spectrum of **M7** (*m*/*z* 555) at CE = 20 eV.

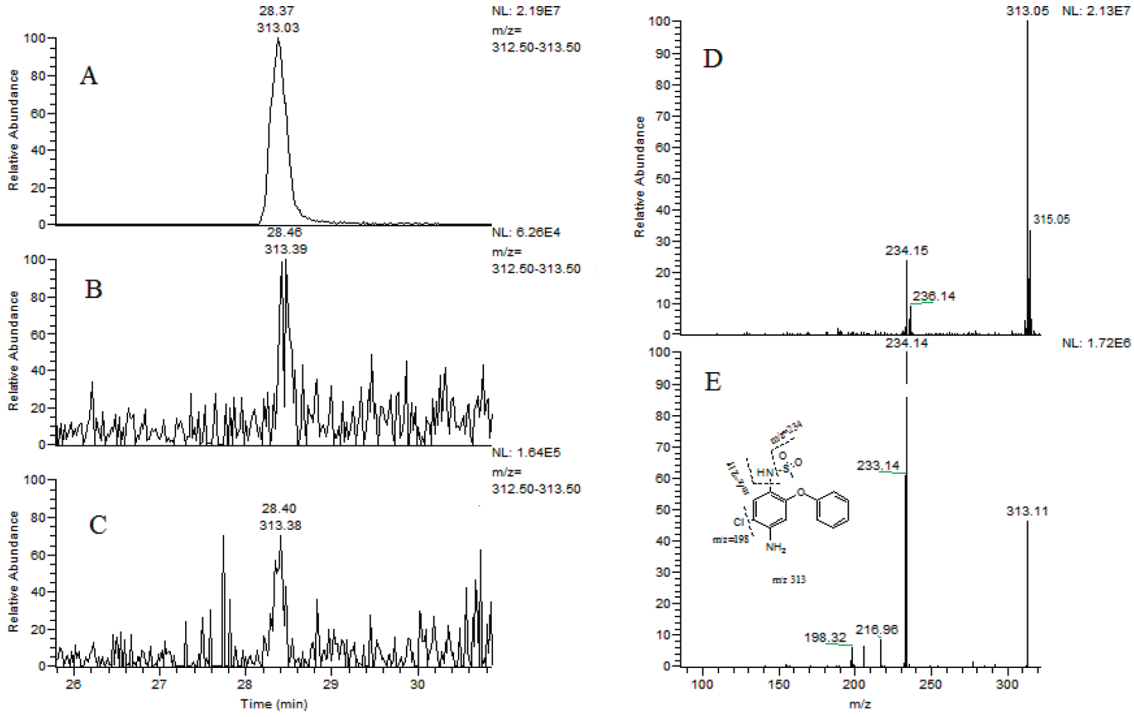

Figure 3. Identification of **M8** (*m*/*z* 313). (A) LC−MS chromatogram of synthetic standard **M8** with $[MH]^+$ extracted for the ion at *m*/*z* 313. (B) LC−MS chromatogram of **M8** at *m*/*z* 313 in MPO and **M1** incubation solutions. (C) LC−MS chromatogram of **M8** in HOCl and **M1** reaction product. (D) Full mass spectrum of **M8** (*m*/*z* 313). (E) LC−MS/MS spectrum of **M8** (*m*/*z* 313) at CE = 35 eV.

mixtures. Aliquots were removed from the incubation mixtures, and the reaction was quenched at various time points by the addition of ice-cold acetonitrile. The amount of 3-chloroprocainamide formation at different time points was monitored.

Results

Bioactivation of Nimesulide by MPO. Nimesulide does not undergo facile metabolism when incubated with MPO either in the presence or in the absence of a biological nucleophile such as NAC. However, in the presence of NAC, a trace amount of reduced nimesulide−NAC conjugate **M3** with an ion at *m*/*z* 440 with a retention time of 27.7 min was detected in a manner similar to the HLM-mediated metabolism of nimesulide as reported previously (*9*). Nimesulide is difficult to ionize under the mass spectrometry conditions utilized in these experiments, and standard calibration curves could be not obtained at low concentrations. Thus, quantitative measurement of nimesulide consumption mediated by MPO in the presence of NAC was not accurately quantified and assumed to be less than 0.5% of the total nimesulide concentration.

Bioactivation of Reduced Nimesulide by MPO. Reduced nimesulide **M1** underwent more efficient metabolism upon incubation with MPO than nimesulide at 37 °C. The observed half-life of **M1** with MPO was ∼5 h. The two main observable metabolites from the incubation mixtures were **M7**, a reduced nimesulide dimer at *m*/*z* 555 with a t_R of 29.5 min as the major metabolite (Figure 2), and **M8**, a monochlorinated derivative at *m*/*z* 313 with a t_R of 28.4 min as the minor metabolite (Figure 3). In addition, metabolites **M5A** (Scheme 2) at *m*/*z* 295 and **M5C** at *m*/*z* 293 were observed occasionally to a lesser extent as detected by LC−MS analysis (presumably because of its reactive nature). MS/MS analysis of **M5A** showed that it was the hydroxylamine derivative of **M1** and not a phenoxy ring or hydroxylated **M1** generated through a P450 arene oxidation. The structure of dimer **M7** was proposed on the basis of MS/MS analysis and established by comparison with a chemically synthesized standard (by oxidizing **M1** in the presence of dichloroamine B). The dominant fragment ion of **M7** was *m*/*z* 476 (for the loss of SO_2CH_3). The structure of **M7** was characterized by ^{1}H NMR (Figure 4) and ^{13}C NMR spectroscopy. In coelution experiments, a synthetic standard and **M7** had the same retention time and MS/MS fragmentation pattern (Figure 2). **M8** exhibited a typical (M:M + 2) 3:1 isotopic pattern in the total ion mass spectrum, indicating for a chlorine atom inclusion in the structure. MS/MS analysis of **M8** at *m*/*z* 313 presented fragment ions at *m*/*z* 234 (100%, loss of 79 for SO_2CH_3), *m*/*z* 216 (10%, loss of $NHSO_2CH_3$), and *m*/*z* 198 (8%, loss of Cl). Formation of **M8** was confirmed from the coelution experiments with the chemically synthesized standard (Figure 3). Structural assignments for **M8** by ^{1}H NMR are shown in Figure 5 and further confirmed by ^{13}C NMR. On the basis of their MS/MS fragmentation, metabolite **M5A** (*m*/*z* 295) was proposed as the N-hydroxylated (and partially reduced) nimesulide and **M5C** was proposed as the nitroso (N═O) metabolite.

When reduced nimesulide **M1** was incubated with MPO in the presence of NAC, a few additional metabolites were identified apart from the **M1**−NAC conjugate **M3** (*m*/*z* 440) (observed from HLM incubations) and monochlorinated **M8** (*m*/*z* 313) metabolites as mentioned above. The new metabolites detected from these incubations were **M4** (*m*/*z* 456), **M6** (*m*/*z* 585), and **M9** (*m*/*z* 422) at retention times of 25.9, 29.3, and 25.6 min, respectively. Metabolites **M4** and **M6** were purified by preparative HPLC analysis.

The MS/MS analysis of metabolite **M4** revealed fragment ions at *m*/*z* 377 (∼26%) indicating a loss of 79 characteristic of the SO_2CH_3 group and *m*/*z* 279 for the loss of a NAC-*S*-oxide fragment as shown in Figure 6. Further, via comparison of panels C and D of Figure 6, we concluded that **M4** from the MPO metabolism study had a MSMS fragmentation pattern different from that of the hydroxylated **M1**−NAC adduct (*m*/*z* 456) we reported previously from the HLM metabolism studies. **M4** appeared to arise from further oxidation of NAC-conjugated

Scheme 2. Identified Metabolites of Reduced Nimesulide

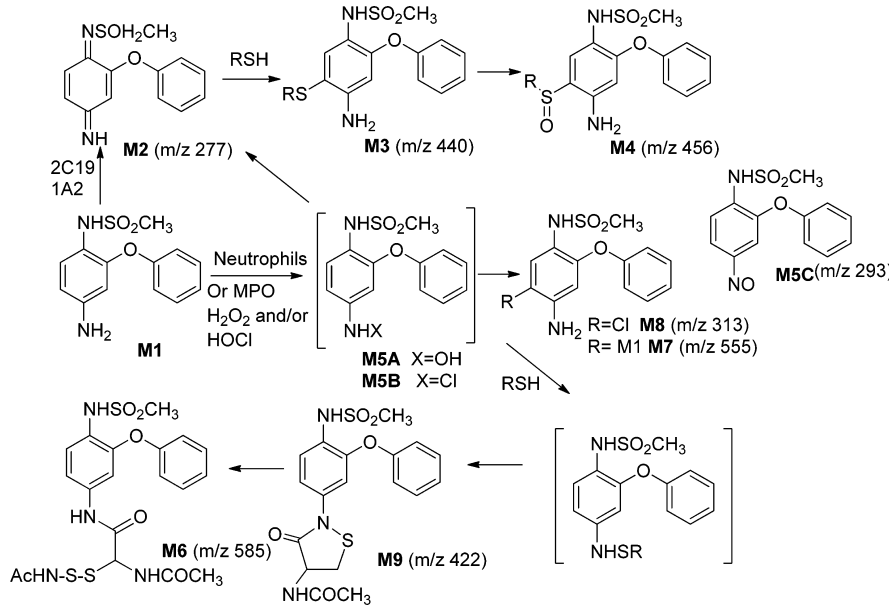

metabolite **M3** and only presented in MPO incubation samples. The structure of **M4** was confirmed by chemical synthesis and coelution experiments. The ^{1}H NMR data of **M4** were similar to the **M3** NMR data, except that peaks for the methylene group (CH_2) were shifted downfield from 3.00 and 3.22 ppm in conjugate **M3** to 3.54 and 3.77 ppm in **M4**, respectively. These shifts represented oxidation of the sulfur atom. In addition, the ^{1}H NMR spectrum indicated that the sample was a mixture of two diastereomers presenting two singlets for the $COCH_3$ group and the $NHSO_2CH_3$ group, due to the formation of a diastereomeric chiral sulfoxide.

Metabolite **M6** was the major component in the incubations (Figure 7). MS/MS analysis of **M6** exhibited fragment ions at *m/z* 506 (−79 due to the apparent loss of the SO_2CH_3 group), 307 (−278 due to the loss of a reduced nimesulide moiety), and 278 (−307 due to the loss of the NAC dimer portion of the proposed structure).

The ^{1}H NMR spectrum of **M6** had structural features indicating possibly two NAC molecules were conjugated with one molecule of reduced nimesulide. In addition, the typical aromatic protons of reduced nimesulide at 6.2 and 6.4 ppm were shifted downfield at 7.28 ppm. Two sharp singlets at 1.96 and 1.97 ppm confirmed two NAC molecules were associated with metabolite **M6**. The structure for **M6** was assigned as shown in Figure 8 by taking into account all data and confirmed by its chemical synthesis followed by coelution experiments.

Metabolite **M9** was the minor metabolite, and its structure was proposed on the basis of MS/MS data exhibiting daughter ions at *m/z* 343 (65%, loss of 79 for SO_2CH_3), *m/z* 335 (100%, loss of 87 C_4H_7NO fragment), and *m/z* 310 (50% loss of 112 for $C_5H_6NO_2$ fragment) (Figure 9).

Oxidation of M1 by HOCl. In situ oxidation of reduced nimesulide with HOCl generated from NaOCl and H_2O_2 provided a metabolism pattern similar to that observed with MPO. In the absence of NAC, metabolites **M7**, **M8**, and **M5C** were detected in good quantities; in the presence of NAC, the major metabolites were still **M3** along with **M6** and **M8**.

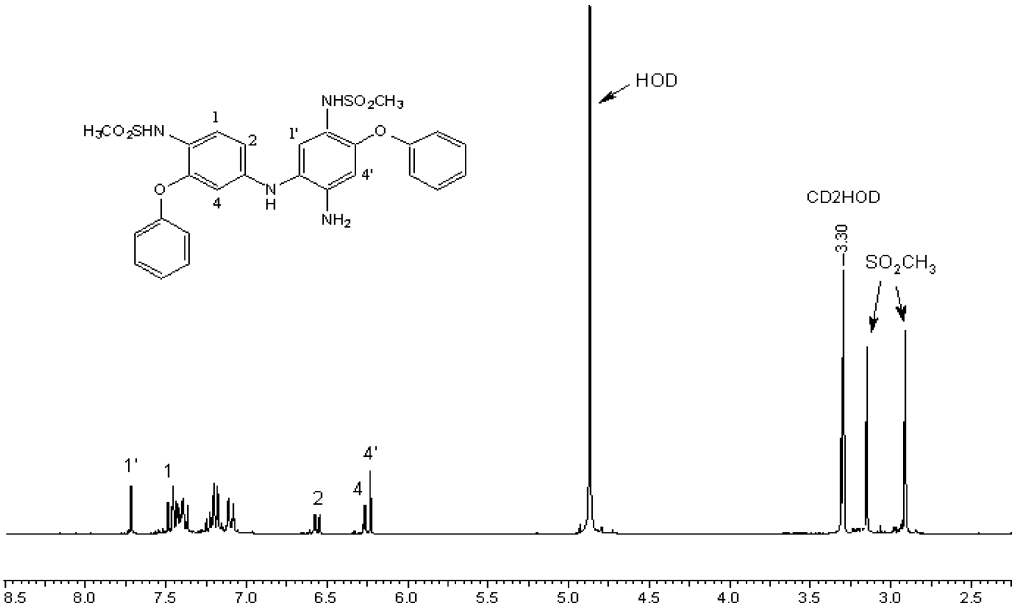

Figure 4. ^{1}H NMR spectrum of **M7**.

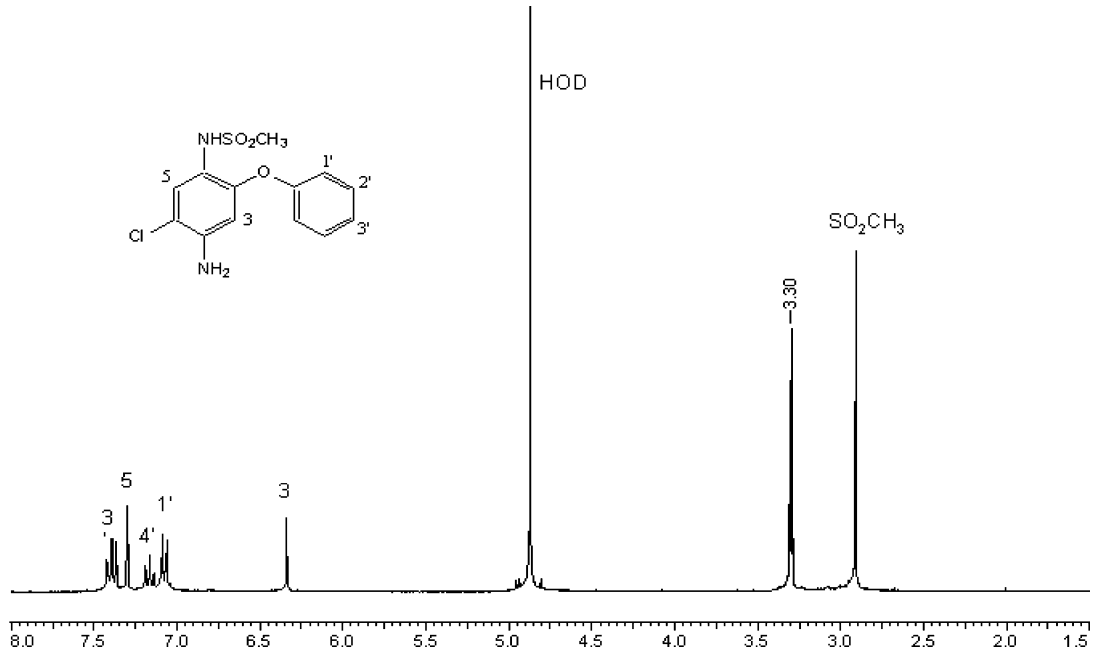

Figure 5. ^{1}H NMR spectrum of **M8**.

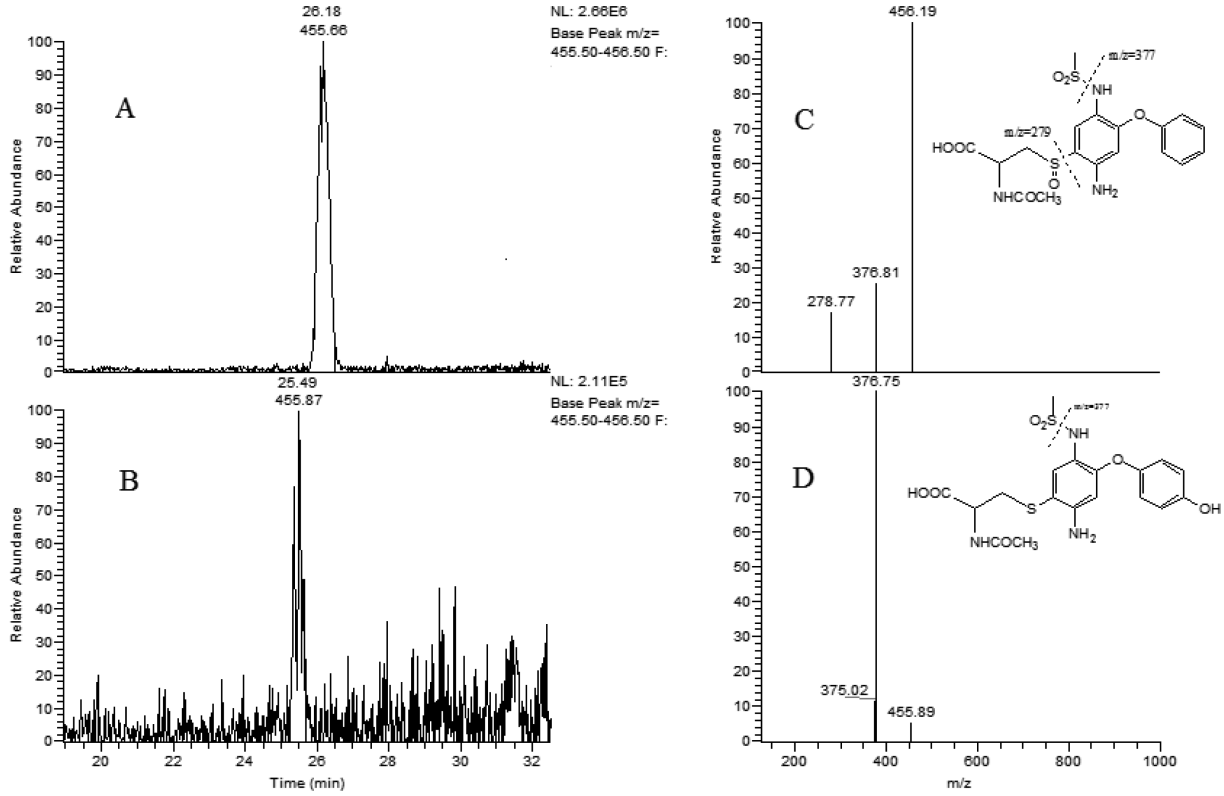

Figure 6. Characterization of metabolite **M4** (*m*/*z* 456). (A) LC chromatogram filtered for the ion at *m*/*z* 456 in **M1** and MPO incubation sample. (B) LC chromatogram filtered for the ion at *m*/*z* 456 in the **M1** and HLM incubation sample. (C) MS/MS spectrum of the ion at *m*/*z* 456 in the **M1** and MPO incubation sample. (D) MS/MS spectrum of the ion at *m*/*z* 456 in the **M1** and HLM incubation sample.

Inhibition of MPO by M1. Procainamide is oxidized to 3-chloroprocainamide efficiently by MPO (*23*). **M1** was first incubated with MPO for 15 min, and then procainamide was added. The oxidizing activity of MPO was evaluated by monitoring the rate of formation of 3-chloroprocainamide in the presence and absence of **M1** (control). The data obtained indicated that preincubation of MPO with **M1** for 15 min led to a decrease in the rate of formation of 3-chloroprocainamide compared to the control (Figure 10). On the basis of the observed data, we hypothesized that **M1** exhibits mechanism-based inactivation of MPO.

Bioactivation of Nimesulide and M1 by Neutrophils. Incubation of nimesulide with or without in vitro activation of neutrophils for 2 h revealed virtually no metabolism. Nimesulide was observed to remain stable by LC−MS analysis. Reduced nimesulide **M1** on the other hand when incubated in vitro with activated or nonactivated neutrophils had a half-life of ∼6 h. With nonactivated neutrophils, a variety of metabolites were

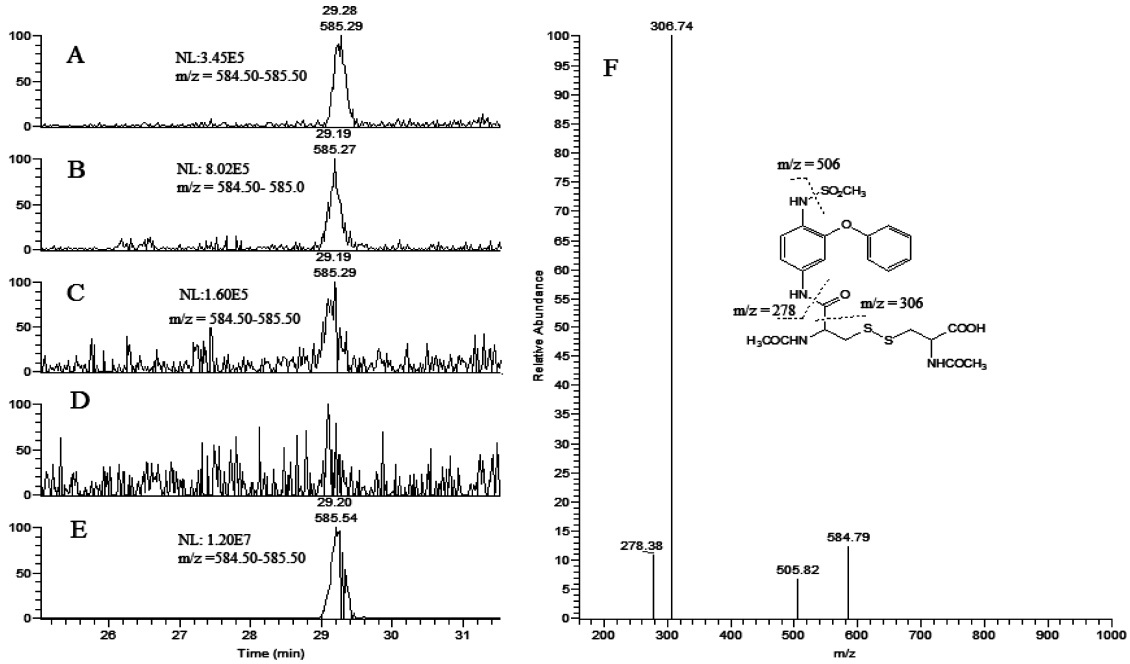

Figure 7. Identification of **M6** (*m*/*z* 585). (A) LC−MS chromatogram of **M6** in HOCl and **M1** reaction product with $[MH]^+$ extracted for the ion at *m*/*z* 585. (B) LC−MS chromatogram of **M6** for the ion at *m*/*z* 585 in MPO and **M1** incubation solutions. (C) LC−MS chromatogram of **M6** in neutrophil and **M1** incubation solutions. (D) LC−MS chromatogram of **M6** in HLM and **M1** incubation solutions. (E) LC−MS chromatogram of synthetic standard **M6**. (F) LC−MS/MS spectrum of **M6** (*m*/*z* 585) at CE = 25 eV.

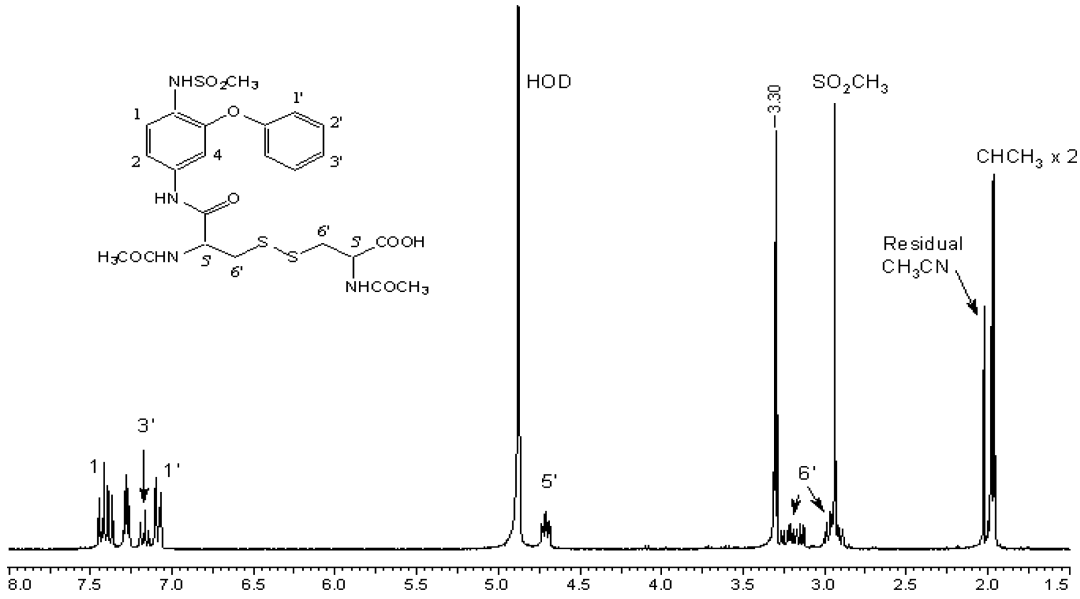

Figure 8. ^{1}H NMR spectrum of **M6**.

apparent in the presence of *N*-acetylcysteine (NAC) and **M1**. These were identified as **M3** (*m*/*z* 440), **M4** (*m*/*z* 456), and **M5C-NAC** (*m*/*z* 454). With activated neutrophils, **M6** (*m*/*z* 585) was observed, in addition to the metabolites mentioned above.

Comparison of Reduced Nimesulide Metabolism by P450 and HRP with MPO. To determine whether P450 enzymes and HRP oxidize **M1** to **M6**, cDNA-expressed human P450 enzymes (1A1, 1A2, 3A4, 2C9, 2C19, 2D6, and 2E1) were incubated with **M1**, and the formation of adduct **M6** was monitored by LC−MS. However, only MPO and activated neutrophiles exhibited a high efficiency of oxidation for reduced nimesulide **M1**. **M6** was not observed with HLM, P450s, and HRP (Figure 11). This suggests **M1** may undergo a different pathway of N-activation by MPO compared with P450s and HRP.

Discussion

The molecular mechanisms underlying the idiosyncratic hepatotoxicity of nimesulide remain unknown, and animal models that can allow exploration of the mechanisms are not well developed (*24, 25*). Several hypotheses have been proposed to contribute to the toxicity, including oxidative stress, covalent protein binding, and mitochondrial injury (*7*). The hepatic metabolism and disposition of nimesulide and its metabolites have also been proposed to play a critical role in mediating the toxicity (*12*). In previous studies by this lab, we have provided evidence that a known reduced nimesulde metabolite in humans, termed **M1**, can undergo subsequent oxidation to a potent electrophilic species, a diiminoquinone intermediate that is capable of subsequent conjugation with *N*-acetylcysteine (NAC) and human serum albumin (HSA). Although the reduced

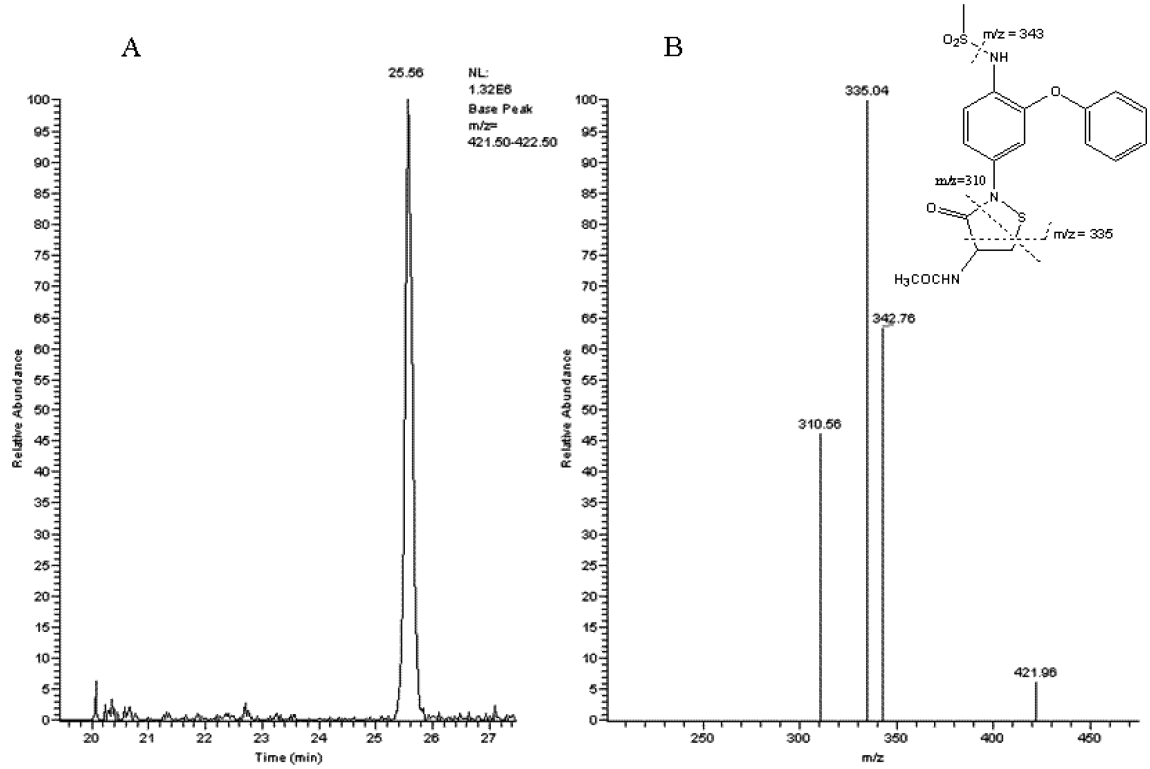

Figure 9. Identification of **M9** (*m*/*z* 422). (A) LC−MS chromatogram of **M9** in MPO and **M1** incubation solutions with $[MH]^+$ extracted for the ion at *m*/*z* 422. (B) LC−MS/MS spectrum of **M9** (*m*/*z* 422) at CE = 25 eV.

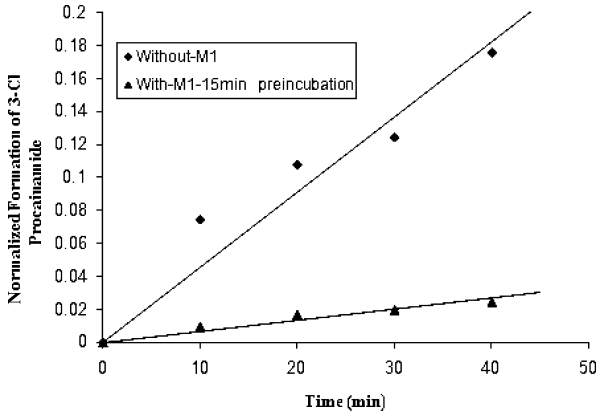

Figure 10. Production of 3-chloroprocainamide from MPO and procainamide in the absence and presence of 10 μM **M1** at different time points.

nimesulide metabolite, **M1**, has not been studied in vivo or shown to bind to biological macromolecules in vivo, [^{14}C]-nimesulide has been shown to bind to HLM or immortalized human hepatocytes (HC-04) in vitro, lending support to the hypothesis that this metabolite may lead to reactive intermediate formation and subsequent protein covalent binding (*26*). Thus, we hypothesize that the reactive diiminoquinone intermediate generated from oxidation of the nimesulide metabolite, **M1**, may contribute importantly to the idiosyncratic toxicity of nimesulide. In this work, we have examined the potential for MPO and neutrophils to mediate this proposed pathway of **M1** bioactivation in vitro.

MPO has been shown by a number of research groups to provide an alternative to P450-mediated bioactivation of a number of substrates with low redox potentials (*27, 28*). MPO is produced by activated mammalian neutrophils when recruited to sites of inflammation and plays an important antimicrobial role in killing pathogens, because of its ability to catalyze peroxide-mediated oxidation of halide ions. Pattison et al. (*27*) have demonstrated in their human inflammatory disease model that the presentation of a pro-electrophilic species, like **M1**, at the site of inflammation can lead to MPO-mediated oxidation. The mechanism of MPO-mediated oxidation of amine-containing compounds is distinct from that of P450s and can generate unique *N*-chloroamine, nitroso, *N*-hydroxy, and/or nitrone species when compared with other enzyme-mediated oxidative pathways.

We have demonstrated in these studies that MPO can bioactivate the amine group of reduced nimesulide by indentifying several reactive species capable of generating stable metabolites such as **M8**, **M6**, and **M9**. In addition, the MPO-mediated metabolic pathway produced activated metabolites that were different from those of the HLM-mediated pathway. The difference between the oxidative pathways can be illustrated by the generation of metabolites **M6** and **M9**. The mechanism of formation of metabolite **M6** is proposed in Figure 12. As shown in the figure, **M1** is proposed to undergo a sequence involving N-chlorination/hydroxylation, NAC addition, intramolecular cyclization, and subsequently addition of a second NAC moiety to form **M6**. The identification of **M9** is consistent with and provides support for this pathway.

The identification of **M8**, generated by a proposed intramolecular chlorine atom transfer process from an N-chlorinated metabolite **M5B**, provides additional evidence of differences in the HLM- and MPO-mediated pathways. In the absence of NAC, **M5B** may undergo facile elimination of HCl to form the diiminoquinone or conjugation with unreacted **M1** to form the dimer **M7**. In the presence of NAC, **M5B** produces the conjugate **M3**, as reported earlier. The coelution data from the HLM- and MPO-mediated incubations are presented as Supporting Information. Formation of **M8** was independently confirmed by in situ studies with NaOCl and H_2O_2. The intramolecular transfer of a chlorine atom from a nitrogen atom

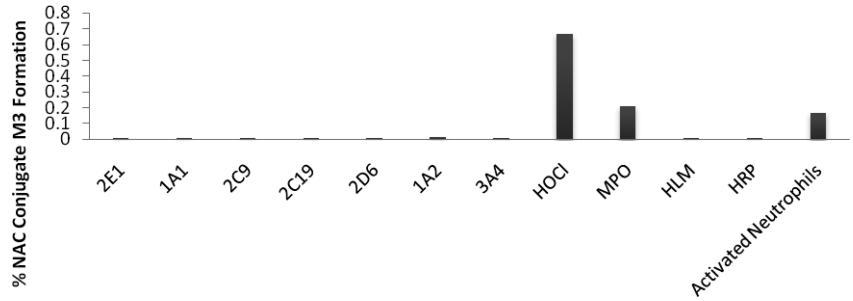

Figure 11. Formation of **M6** by P450 enzymes, HRP, MPO, and activated neutrophils.

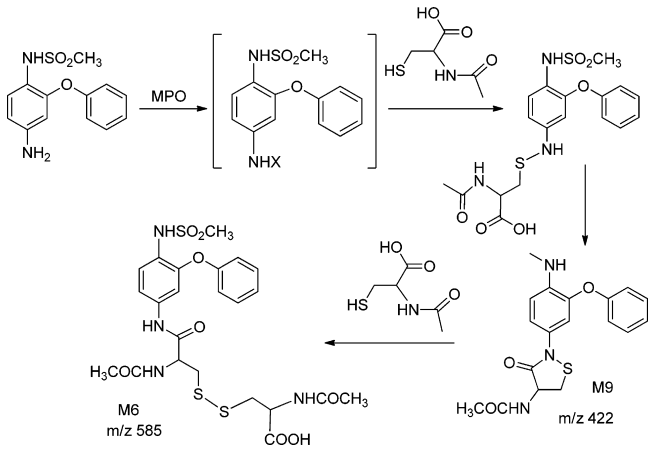

Figure 12. Proposed mechanism for the formation of **M6** at *m/z* 585.

to aromatic carbon is well-recognized (*23, 29*). It is worth mentioning here that the diiminoquinone species does not appear sufficiently reactive toward nucleophilic addition of chloride ion to form the aromatic chloro metabolite, **M8**, via such a pathway. Metabolite **M8** was not detectable in the incubations either with HLMs or without MPO, further implying that MPO-mediated activation is critical.

The in vitro evidence provided here demonstrates the activation of nitrogen to reactive *N*-chloro, *N*-hydroxy, or nitrogen-based radical species, which is capable of conjugating with biological nucleophiles, such as NAC, at the inflammation site in a specific manner where neutrophils are activated and significant quantities of MPO are localized. Nimesulide is susceptible to nitro oxido-reductase enzymes to produce reduced nimesulide, which can undergo further activation by MPO in the presence of NAC (data not shown). The possibility that MPO can activate the reduced nimesulide to electrophilic species capable of conjugating with macromolecules suggests that the irreversible modification of these macromolecules may be a potential trigger for inducing toxicity. In addition, irreversible inactivation of MPO as shown in Figure 10 by reduced nimesulide may interfere with the metabolism of other drugs (toxicity induced by drug−drug interaction). These observations provide support for the potential for idiosyncratic hepatotoxicity occurring through neutrophil-mediated MPO generation and its action on the amine group of reduced nimesulide to produce reactive species capable of reacting with tissue macromolecules. Scheme 2 depicts further advancement in our understanding of metabolism and bioactivation of nimesulide and its metabolite **M1** by MPO.

In conclusion, we provide evidence that supports arylamine activation of reduced nimesulide by neutrophils and MPO in generating reactive nitrogen-based species as demonstrated by the identification and characterization of metabolites **M6**, **M8**, and **M9**. The structures of metabolites **M6** and **M8** were independently confirmed by chemical synthesis, and mechanisms for the formation of **M6**, **M8**, and **M9** are proposed. The activation of the aromatic amine group by MPO, followed by the irreversible conjugation with NAC, is a model for the possibility of conjugation with biological macromacromolecules that could potentially trigger hepatotoxicity in vivo. However, more work is clearly needed to establish the molecular mechanisms underlying the observed hepatotoxicity associated with nimesulide therapy.

Supporting Information Available: LC−MS data of the *m/z* 440 adduct. This material is available free of charge via the Internet at http://pubs.acs.org.

References

(1) Tan, H., Ong, W. M. C., Lai, S. H., and Chow, W. C. (2007) Nimesulide-induced hepatotoxicity and fatal hepatic failure. *Singapore Med. J. 48*, 582–585.
(2) Dastis, S. N., Rahier, J., Lerut, J., and Geubel, A. P. (2007) Liver transplantation for nonsteroidal anti-inflammatory drug-induced liver failure: Nimesulide as the first implicated compound. *Eur. J. Gastroenterol. Hepatol. 19*, 919–922.
(3) Macia, M. A., Carvajal, A., del Pozo, J. G., Vera, E., and del Pino, A. (2002) Hepatotoxicity associated with nimesulide: Data from the spanish pharmacovigilance system. *Clin. Pharmacol. Ther. 72*, 596–597.
(4) Steenbergen, W. V., Peeters, P., Bondt, J. D., Staessen, D., Buscher, H., Laporta, T., Roskams, T., and Desmet, V. (1998) Nimesulide-induced acute hepatitis: Evidence from six cases. *J. Hepatol. 29*, 135–141.
(5) Traversa, G., Bianchi, C., Da Cas, R., Abraha, I., Menniti-Ippolito, F., and Venegoni, M. (2003) Cohort study of hepatotoxicity associated with nimesulide and other non-steroidal anti-inflammatory drugs. *Br. Med. J. 327*, 18–22.
(6) Rainsford, K. D. (2006) Current status of the therapeutic uses and actions of the preferential cyclo-oxygenase-2 NSAID, nimesulide. *Inflammopharmacology 14*, 120–137.
(7) Boelsterli, U. A. (2002) Mechanisms of NSAID-induced hepatotoxicity: Focus on nimesulide. *Drug Saf. 25*, 633–648.
(8) Bernareggi, A. (1998) Clinical pharmacokinetics of nimesulide. *Clin. Pharmacokinet. 4*, 247–274.
(9) Li, F., Chordia, M. D., Huang, T., and Macdonald, T. L. (2009) *In vitro* nimesulide studies toward understanding idiosyncratic hepatotoxicity: Diiminoquinone formation and conjugation. *Chem. Res. Toxicol. 22*, 72–80.
(10) Obach, R. S., and Dalvie, D. K. (2006) Metabolism of nomifensine to a dihydroisoquinolonium ion metabolite by human myeloperoxidase, hemoglobin, monoamine oxidase A and cytochrome P450 enzymes. *Drug Metab. Dispos. 34*, 1310–1316.
(11) Reilly, T. P., Woster, P. M., and Svensson, C. K. (1999) Methemoglobin formation by hydroxylamine metabolites of sulfamethoxazole and dapsone: Implications for differences in adverse drug reactions. *J. Pharmacol. Exp. Ther. 288*, 951–959.
(12) Boelsterli, U. A., Ho, H. K., Zhou, S. F., and Leow, K. Y. (2006) Bioactivation and hepatotoxicity of nitroaromatic drugs. *Curr. Drug Metab. 7*, 715–727.
(13) Lu, W., and Uetrecht, J. P. (2008) Peroxidase mediated bioactivation of hydroxylated metabolites of carbamazepine and phenytoin. *Drug Metab. Dispos. 36*, 1624–1636.

(14) Miyamoto, G., Zahid, N., and Uetrecht, J. P. (1997) Oxidation of dichlofenac to reactive intermediates by neutrophils, myeloperoxidase and hypochlorus acid. *Chem. Res. Toxicol. 10*, 414–419.
(15) Uetrecht, J. (2002) N-oxidation of drugs associated with idiosyncratic drug reactions. *Drug Metab. Rev. 34*, 651–665.
(16) Gardner, I., Popovic, M., Zahid, N., and Uetrecht, J. P. (2005) A comparison of the covalent binding of clozapine, procainamide, and vesnarinone to human neutrophils in vitro and rat tissues in vitro and in vivo. *Chem. Res. Toxicol. 18*, 1384–1394.
(17) Hofstra, A. H., and Uetrecht, J. P. (1993) Myeloperoxidase-mediated activation of xenobiotics by human leukocytes. *Toxicology 82*, 221–242.
(18) Pirmohamed, M., Madden, S., and Park, B. K. (1996) Idiosyncratic drug reactions: Metabolic bioactivation as a pathogenic mechanism. *Clin. Pharmacokinet. 31*, 215–230.
(19) van der Veen, B. S., de Winther, M. P. J., and Heeringa, P. (2009) Myeloperoxidase: Molecular mechanisms of action and their relevance to human health and disease. *Antioxid. Redox Signaling 11*, 2899–2937.
(20) Lai, W. G., Zahid, N., and Uetrecht, J. P. (1999) Metabolism of trimethoprim to a reactive iminoquinone methide by activated human neutrophils and hepatic microsomes. *J. Pharmacol. Exp. Ther. 291*, 292–299.
(21) Klebanoff, S. J. (1970) Myeloperoxidase: Contribution to the microbicidal activity of intact leukocytes. *Science 169*, 1095–1097.
(22) Ferrantei, A., and Thong, Y. H. (1980) Simultaneous preparation of mononuclear and polymorphonuclear leukocytes from horse blood on Ficoll-Hypaque medium. *J. Immunol. Methods 34*, 279–285.
(23) Uetrecht, J. P., and Zahid, N. (1991) N-Chlorination and oxidation of procainamide by myeloperoxidase: Toxicological implications. *Chem. Res. Toxicol. 4*, 218–222.
(24) Ong, M. M. K., Wong, A. S., Leow, K. Y., Khoo, Y. M., and Boelsterli, U. A. (2006) Nimesulide induced hepatic mitochondrial injury in heterozygous sod2$^{+/-}$ mice. *Free Radical Biol. Med. 40*, 420–429.
(25) Moreno, A. J., Oliveira, P. J., Nova, C. D., Alvaro, A. R., Moreira, R. A., Santos, S. M. D., and Macedo, T. (2007) Unaltered hepatic oxidative phosphorylation and mitochondrial permeability transition in Wistar Rats treated with nimesulide: Relevance for nimesulide toxicity characterization. *J. Biochem. Mol. Toxicol. 21*, 53–61.
(26) Kale, V., Hsiao, C. J., and Boelsterli, U. A. (2010) Nimesulide-induced electrophile stress activates Nrf2 in human hepatocytes and mice but is not sufficient to induce hepatotoxicity in Nrf2-deficient mice. *Chem. Res. Toxicol. 23*, 967–976.
(27) Pattison, D. I., and Davies, M. J. (2006) Reactions of myeloperoxidase-derived oxidants with biological substrates: Gaining chemical insight into human inflammatory diseases. *Curr. Med. Chem. 13*, 3271–3290.
(28) Sun, Q., Zhu, R., Foss, F. W., and Macdonald, T. L. (2008) In vitro metabolism of a model cyclopropylamine to reactive intermediate: Insights into trovafloxacin-induced hepatotoxicity. *Chem. Res. Toxicol. 21*, 711–719.
(29) Uetrecht, J. P., Shear, N. H., and Zahid, N. (1993) N-Chlorination of sulfamethoxazole and dapsone by the myeloperoxidase system. *Drug Metab. Dispos. 21*, 830–834.

TX1001496